

E. Musso*

AN EXPERIMENTAL STUDY OF GOLDSTEIN–PETRICH CURVES

Abstract. Numerical methods are used to prove the existence of closed embedded curves in \mathbb{R}^2 and \mathbb{H}^2 whose shapes are invariant under the Goldstein–Petrich flow. Numerical routines are used to compute all closed spherical free elasticae. The evidence of the experiments shows the existence of a unique, up to rotations, embedded closed free elastica of S^2 with symmetry group of order h , for every positive integer $h \geq 2$. The order of the symmetry groups and the number of self-intersection points of any closed free elastica in S^2 are determined.

1. Introduction

The interplay between integrable evolution equations and the motion of curves has been the focus of intense research in the past decades, both in geometry and mathematical physics (see for instance [6, 7, 8, 4, 11, 12, 14, 15, 16, 20, 21, 23] and the literature therein). In the seminal paper [11], Goldstein and Petrich related the mKdV hierarchy to the motions of curves in the plane. Later, this approach has been generalized to other 2-dimensional Klein geometries [6, 7, 8] or to higher-dimensional homogeneous spaces [20, 21]. The second Goldstein–Petrich flow for curves in a 2-dimensional Riemannian space form S_ε^2 of constant curvature $\varepsilon = 0, 1, -1$, is defined by the *modified Korteweg–de Vries* equation

$$(1) \quad \kappa_t + \kappa_{sss} + \frac{3}{2}\kappa^2\kappa_s = 0,$$

where $\kappa(s, t)$ denotes the (geodesic) curvature. Closed curves whose shape is invariant under the flow defined by (1) are referred to as *Goldstein–Petrich* curves. In this case, $\kappa(s, t)$ must be a periodic solution of (1) in the form of a traveling wave, so $\kappa = \kappa(s + (\varepsilon - \lambda)t)$ and

$$(2) \quad \kappa_{ss} + \frac{\kappa^3}{2} + (\varepsilon - \lambda)\kappa = \mu,$$

where μ is a constant of integration. On physical and geometrical grounds it is natural to demand that the curves are closed and without self intersections. Generic periodic solutions of (2) need not correspond to closed curves [23]. And, even if κ corresponded to a closed curve, in general there would be points of self-intersection. It is known that, in the spherical case, there exists a countable family of simple Goldstein–Petrich curves, with $\mu = 0$ [2, 17]. These particular solutions are known as *elastic curves* and they constitute a classical topic in mathematical physics and geometry. However, in the

*This research was partially supported by the MIUR project *Geometria delle varietà differenziabili*, and by the group GNSAGA of the INdAM

Euclidean or hyperbolic case, closed elasticæ always have self intersections [2, 17, 23]. It is then a natural problem to look for numerical procedures to recognize whether or not there exist simple closed Goldstein–Petrich planar or hyperbolic curves. Another natural problem is to develop effective computational methods to find all simple closed elasticæ in the 2-sphere.

On the base of our numerical approach, we exhibit explicit examples of simple Goldstein–Petrich curves in the Euclidean plane and in the Poincaré disk. Experimental evidences confirm the existence of 1-parameter families of simple closed Goldstein–Petrich curves with symmetry groups \mathbb{Z}_n , for every $n \in \mathbb{N}$. In the second part of the paper we examine free elasticæ in S^2 . The curvature can be expressed in term of the Jacobi elliptic function $\text{cn}(-, \sqrt{\lambda})$, $\lambda \in (0, 1/2)$. We compute the monodromy of the spin Frenet system and we construct a map $\phi : \mathbb{Q} \cap (0, 1/2) \rightarrow (0, 1/2)$ such that $\lambda = \phi(p/q)$ gives a closed elastica. Every closed spherical elastica arises in this fashion, for some $p/q \in \mathbb{Q} \cap (0, 1/2)$. Our tests suggest that if $\lambda = \phi(p/2q)$ then the corresponding elastica has symmetry group \mathbb{Z}_q and possesses $(p - 1)q$ points of self intersection. In particular, if $p = 1$ we obtain a simple closed elastica with symmetry group \mathbb{Z}_q , for every $q \geq 2$. If $\lambda = \phi(p/(2q + 1))$ then the curve has symmetry group \mathbb{Z}_{2q+1} and possesses $(2p - 1)(2q + 1)$ points of self intersection. As an application we compute and visualize embedded Pinkall’s tori in \mathbb{R}^3 with non trivial symmetry groups \mathbb{Z}_n , for every $n \in \mathbb{N}$ [26].

Acknowledgments. Numerical computations and visualization have been performed with the software *Mathematica 6*.

2. Goldstein–Petrich curves

2.1. Frames

We let \mathbb{R}_ε^3 , $\varepsilon = -1, 0, 1$, be the real 3-dimensional space with coordinates (x^1, x^2, x^3) endowed with the bilinear form

$$\langle \mathbf{x}, \mathbf{y} \rangle_\varepsilon = \varepsilon x^1 y^1 + x^2 y^2 + x^3 y^3 = {}^t \mathbf{x} g^\varepsilon \mathbf{x}$$

and with the orientation $dx^1 \wedge dx^2 \wedge dx^3 > 0$. If $\varepsilon = -1$ we also fix a time-orientation by saying that a null-vector \mathbf{x} is future-directed if $x^1 > 0$. We denote by $S_\varepsilon^2 \subset \mathbb{R}_\varepsilon^3$ the space-like 2-dimensional submanifolds

$$\begin{cases} S_1^2 &= \{ \mathbf{x} \in \mathbb{R}_1^3 : \|\mathbf{x}\|_1^2 = 1 \} \cong S^2, \\ S_{-1}^2 &= \{ \mathbf{x} \in \mathbb{R}_{-1}^3 : \|\mathbf{x}\|_{-1}^2 = -1, x^1 \geq 1 \} \cong \mathbb{H}^2, \\ S_0^2 &= \{ \mathbf{x} \in \mathbb{R}_0^3 : x^1 = 1 \} \cong \mathbb{R}^2. \end{cases}$$

We indicate by $\text{SO}_\varepsilon(3)$ the connected component of the identity of the automorphism group of \mathbb{R}_ε^3 . It is convenient to think of $\text{SO}_\varepsilon(3)$ as the frame manifold of all oriented basis $\mathbf{a} = (\mathbf{a}_1, \mathbf{a}_2, \mathbf{a}_3)$ of \mathbb{R}_ε^3 such that $\langle \mathbf{a}_i, \mathbf{a}_j \rangle = g_{ij}^\varepsilon$. If $\varepsilon = -1$ we also require that \mathbf{a}_1 is future-directed. We then let $\mathfrak{so}_\varepsilon(3)$ be the Lie algebra of $\text{SO}_\varepsilon(3)$, whose elements are

3×3 matrices of the form

$$\begin{pmatrix} 0 & -\varepsilon y^1 & -\varepsilon y^2 \\ y^1 & 0 & -y^3 \\ y^2 & y^3 & 0 \end{pmatrix}.$$

REMARK 1. The hyperbolic plane S_{-1}^2 is identified with the unit disk Δ endowed with its standard Poincaré metric

$$\frac{4}{(1-x^2-y^2)^2}(dx^2+dy^2)$$

by means of

$$\mathbf{x} \in S_{-1}^2 \rightarrow \left(\frac{x^2}{x^1}, \frac{x^3}{x^1} \right) \in \Delta.$$

Let $\gamma : I \subset \mathbb{R} \rightarrow S_{\varepsilon}^2$ be a regular curve parameterized by the arclength. For each $s \in I$ we set $\mathbf{t}(s) = \gamma'(s)$ and we denote by $\mathbf{n}(s) \in \mathbb{R}_{\varepsilon}^3$ the unique unit vector such that $(\gamma(s), \mathbf{t}(s), \mathbf{n}(s)) \in \text{SO}_{\varepsilon}(3)$. The map

$$F : s \in I \rightarrow (\gamma(s), \mathbf{t}(s), \mathbf{n}(s)) \in \text{SO}_{\varepsilon}(3)$$

is the *Frenet frame field* of γ . It satisfies the *Frenet–Serret equations*

$$\gamma' = \mathbf{t}, \quad \mathbf{t}' = -\varepsilon\gamma + \kappa\mathbf{n}, \quad \mathbf{n}' = -\kappa\mathbf{t}$$

where $\kappa : I \rightarrow \mathbb{R}$ is the *curvature* of γ . The Serret–Frenet equations can be conveniently written in the form

$$(3) \quad F' = F\mathcal{X}(\kappa)$$

where

$$(4) \quad \mathcal{X}(\kappa) = \begin{pmatrix} 0 & -\varepsilon & 0 \\ 1 & 0 & -\kappa \\ 0 & \kappa & 0 \end{pmatrix}.$$

REMARK 2. By the existence and uniqueness of solutions of linear systems of o.d.e. it follows that for every smooth function $\kappa : I \rightarrow \mathbb{R}$ and every $\mathbf{a} \in \text{SO}_{\varepsilon}(3)$ there exists a unique $F : I \rightarrow \text{SO}_{\varepsilon}(3)$ with initial condition $F(0) = \mathbf{a}$ and satisfying (3). For this reason we will simply say that F is a *Frenet frame with curvature* κ .

2.2. Jets, differential functions and total derivatives

We now collect some definitions taken from [24]. The space of n -th order jets of functions $u \in C^{\infty}(\mathbb{R}, \mathbb{R})$ is denoted by $J^n(\mathbb{R}, \mathbb{R})$. The independent variable is s , the dependent variable and its virtual derivatives up to order n are $u, u_{(1)}, \dots, u_{(n)}$. The projective limit of the natural sequence

$$(5) \quad \dots \rightarrow J^n(\mathbb{R}, \mathbb{R}) \rightarrow J^{n-1}(\mathbb{R}, \mathbb{R}) \rightarrow \dots \rightarrow J^1(\mathbb{R}, \mathbb{R}) \rightarrow J^0(\mathbb{R}, \mathbb{R}) \rightarrow \mathbb{R}.$$

is the *infinite jet space*. It is denoted by $\mathbf{J}(\mathbb{R}, \mathbb{R})$. A function

$$\mathbf{W} : \mathbf{J}(\mathbb{R}, \mathbb{R}) \rightarrow \mathbb{R}$$

is said to be a *differential function* if there exists a polynomial $W \in \mathbb{R}[x_0, x_1, \dots, x_n]$ such that

$$\mathbf{W}(\mathbf{u}) = W(u, u_{(1)}, \dots, u_{(n)}),$$

for every $\mathbf{u} = (s, u, u_{(1)}, \dots, u_{(n)}, \dots) \in \mathbf{J}(\mathbb{R}, \mathbb{R})$. The set of the polynomial differential functions will be denoted by $J[\mathbf{u}]$. The total derivative

$$\delta : J[\mathbf{u}] \rightarrow J[\mathbf{u}]$$

is defined by

$$\delta(\mathbf{W})(\mathbf{u}) = \sum_{j=0}^{\infty} \frac{\partial W}{\partial x_j} \Big|_{\mathbf{u}} u_{(j+1)}.$$

A differential function $\mathbf{W} \in J[\mathbf{u}]$ is *exact* if there exist $\mathcal{P}(\mathbf{W}) \in J[\mathbf{u}]$ such that

$$\mathbf{W} = \delta(\mathcal{P}(\mathbf{W})).$$

The *primitive* $\mathcal{P}(\mathbf{W})$ is unique, up to a constant. We use the notation $\int \mathbf{W} ds$ to denote the primitive $\mathcal{P}(\mathbf{W})$ of \mathbf{W} such that $\mathcal{P}(\mathbf{W})|_0 = 0$. If $\kappa : (s, t) \in \mathbb{R}^2 \rightarrow \mathbb{R}$ is a smooth function, we put

$$j_s(\kappa) : (s, t) \in \mathbb{R} \rightarrow (s, \kappa(s, t), \partial_s \kappa|_{(s, t)}, \dots, \partial_s^n \kappa|_{(s, t)}, \dots) \in \mathbf{J}(\mathbb{R}, \mathbb{R}).$$

The *mKdV hierarchy* can be described as follows : let \mathbf{F}_n and \mathbf{G}_n be the differential functions defined by

$$\mathbf{F}_1 = 0, \quad \mathbf{G}_1 = -1, \quad \mathbf{F}_2 = u_{(1)}, \quad \mathbf{G}_2 = -\frac{1}{2}u^2$$

and by

$$\mathbf{F}_n = \delta^2(\mathbf{F}_{n-1}) + u^2 \mathbf{F}_{n-1} + u_{(1)} \int u \mathbf{F}_{n-1} ds, \quad \mathbf{G}_n = - \int u \mathbf{F}_n ds,$$

for every $n \geq 3$. Then, the *n-th member of the mKdV hierarchy* is the evolution equation

$$\kappa_t + (\delta^2(\mathbf{F}_n) + u^2 \mathbf{F}_n - u_{(1)} \mathbf{G}_n) |_{j_s(\kappa)} = 0.$$

2.3. The Goldstein–Petrich flows

Following [11], a *local dynamics* of curves is defined by

$$(6) \quad \partial_t \gamma = \mathbf{U}|_{j_s(\kappa)} \mathbf{t} + \mathbf{V}|_{j_s(\kappa)} \mathbf{n},$$

where $\mathbf{U}, \mathbf{V} \in J[\mathbf{u}]$ are two differential functions and where

$$\mathbf{F}(-, t) : s \in \mathbb{R} \rightarrow \mathbf{F}(s, t) = (\gamma(s, t), \mathbf{t}(s, t), \mathbf{n}(s, t)) \in \mathbf{SO}_\varepsilon(3),$$

and

$$\kappa(-, t) : s \in \mathbb{R} \rightarrow \kappa(s, t) \in \mathbb{R}$$

denote the Frenet frame and the curvature of the evolving curve, respectively. We also assume that $u\mathbf{V}$ is exact. From (6) and (7) we deduce

$$(7) \quad F^{-1}dF = \mathbf{K}|_{j_s(\kappa)}ds + \mathbf{Q}|_{j_s(\kappa)}dt,$$

where

$$\mathbf{K}, \mathbf{Q} : \mathbf{J}(\mathbb{R}, \mathbb{R}) \rightarrow \mathfrak{so}_\varepsilon(3)$$

are the $\mathfrak{so}_\varepsilon(3)$ -valued differential functions

$$(8) \quad \mathbf{K} = \begin{pmatrix} 0 & -\varepsilon & 0 \\ 1 & 0 & -u \\ 0 & u & 0 \end{pmatrix},$$

and

$$(9) \quad \mathbf{Q} = \begin{pmatrix} 0 & -\varepsilon\mathbf{U} & -\varepsilon\mathbf{V} \\ \mathbf{U} & 0 & -\delta(\mathbf{V}) - u\mathbf{U} \\ \mathbf{V} & \delta(\mathbf{V}) + u\mathbf{U} & 0 \end{pmatrix},$$

where \mathbf{U} is a primitive of $u\mathbf{V}$ (i.e. $\delta(\mathbf{U}) = u\mathbf{V}$). The compatibility equation of (7) is

$$(10) \quad \partial_t(\mathbf{K}|_{j_s(\kappa)}) - \partial_s(\mathbf{Q}|_{j_s(\kappa)}) = [\mathbf{K}, \mathbf{Q}]|_{j_s(\kappa)}.$$

An easy inspection shows that (10) is satisfied if and only if

$$(11) \quad \partial_t(\kappa) = (\delta^2(\mathbf{V}) + (u^2 + \varepsilon)\mathbf{V} + u_{(1)}\mathbf{U})|_{j_s(\kappa)}.$$

The *first Goldstein–Petrich flow* is defined by the choice

$$\mathbf{V}_{(1)} = 0, \quad \mathbf{U}_{(1)} = -1.$$

The curvature then evolves according to

$$\partial_t(\kappa) + \partial_s(\kappa) = 0.$$

Thus, the first GP-flow is trivial from a geometrical viewpoint (i.e. every curve evolves by rigid motions). The *second Goldstein–Petrich flow* is given by

$$(12) \quad \mathbf{V}_{(2)} = -u_{(1)}, \quad \mathbf{U}_{(2)} = \varepsilon - \frac{1}{2}u^2,$$

which yields the *mKdV* equation

$$(13) \quad \kappa_t + \kappa_{sss} + \frac{3}{2}\kappa^2\kappa_s = 0.$$

The choice

$$\mathbf{V}_{(3)} = \varepsilon u_{(1)} - u_{(3)} - \frac{3}{2}u^2 u_{(1)}, \quad \mathbf{U}_{(3)} = -\varepsilon^2 + \frac{1}{2}\varepsilon u^2 - \frac{3}{8}u^4 + \frac{1}{2}u_{(1)}^2 - uu_{(2)}$$

gives the *third Goldstein–Petrich flow*. The corresponding evolution equation is the third member

$$\kappa_t + \kappa_{sssss} + \frac{15}{8}\kappa^4 \kappa_s + \frac{5}{2}\kappa_s^3 + 10\kappa\kappa_s\kappa_{ss} + \frac{5}{2}\kappa^2 \kappa_{sss} = 0$$

of the *mKdV* hierarchy.

REMARK 3. More generally, let $\{q_{(h,n)}\}_{1 \leq h \leq n}$ be the sequences defined recursively by

$$\begin{cases} q_{(1,2n)} = -2n, \\ q_{(h,2n)} = (-1)^h (|q_{(h-1,2n-1)}| + |q_{(h,2n-1)}|), & h = 2, \dots, n, \\ q_{(h,2n)} = q_{(2n-h,2n)}, & h = n+1, \dots, 2n-1, \\ q_{(2n,2n)} = 1, \end{cases}$$

and by

$$\begin{cases} q_{(1,2n+1)} = -(2n+1), \\ q_{(h,2n+1)} = (-1)^h (|q_{(h-1,2n)}| + |q_{(h,2n)}|), & h = 2, \dots, n, \\ q_{(h,2n+1)} = -q_{(2n+1-h,2n)}, & h = n+1, \dots, 2n, \\ q_{(2n+1,2n+1)} = -1. \end{cases}$$

Then, we set

$$b_{(0,0)} = 1, \quad b_{(h,n)} = \varepsilon^h q_{(h,n)}, \quad h = 1, \dots, n, \quad n \in \mathbb{N}$$

and we consider the differential functions defined recursively by

$$\mathbf{A}_{(1,n)} = 0, \quad \mathbf{A}_{(2,n)} = -u_{(1)}, \quad n \geq 2$$

and by

$$\mathbf{A}_{(h,n)} = \delta^2(\mathbf{A}_{(h-1,n)}) + (u^2 + \varepsilon)\mathbf{A}_{(h-1,n)} + u_{(1)} \left(\int u \mathbf{A}_{(h-1,n)} ds - b_{(h-2,n-2)} \right),$$

for each $n \geq 3$ and each $h = 2, \dots, n$. If we define $\mathbf{V}_{(n)}$ and $\mathbf{U}_{(n)}$ by

$$\mathbf{V}_{(n)} = \mathbf{A}_{(n,n+1)}, \quad \mathbf{U}_{(n)} = \left(\int u \mathbf{V}_{(n)} ds \right) - b_{(n-1,n-1)}$$

we get the *n-th Goldstein–Petrich flow*, whose corresponding evolution equation is the *n-th* member of the *mKdV* hierarchy.

REMARK 4. If κ is a solution of (11) and if \mathbf{K} and \mathbf{Q} are defined as in (8) and (9) then the 1-form

$$\Theta = \mathbf{K}|_{j_s(\kappa)} ds + \mathbf{Q}|_{j_s(\kappa)} dt$$

fulfils the Maurer-Cartan equation

$$d\Theta + \Theta \wedge \Theta = 0.$$

Thus, by the Cartan-Darboux theorem, there exist $F : \mathbb{R} \times \mathbb{R} \rightarrow \text{SO}_\varepsilon(3)$ such that $F^{-1}dF = \Theta$. The map F is unique up to left multiplication by an element of $\text{SO}_\varepsilon(3)$. If we put $F = (\gamma, \mathbf{t}, \mathbf{n})$, then $\gamma : \mathbb{R}^2 \rightarrow \mathbb{R}_\varepsilon^3$ is the analytical parametrization of the dynamics of a curve evolving according to (6).

REMARK 5. The first three basic distinguished functionals of (13) are

$$\mathfrak{L}_0 = \int ds, \quad \mathfrak{L}_1 = \int k(s) ds, \quad \mathfrak{L}_2 = \int \kappa^2(s) ds.$$

2.4. Goldstein–Petrich curves

Closed trajectories whose shapes are invariant under (13) are called *Goldstein–Petrich curves* of $\mathcal{S}_\varepsilon^2$ (GP-curves for brevity). Solutions of (13) which correspond to Goldstein–Petrich curves are periodic solutions in the form of a traveling wave, so $\kappa = \kappa(s + (\varepsilon - \lambda)t)$, for some constant λ and

$$(14) \quad \kappa''' + \left(\frac{3}{2}\kappa^2 + (\varepsilon - \lambda) \right) \kappa' = 0.$$

Integrating (14) we find

$$(15) \quad \kappa'' + \frac{\kappa^3}{2} + (\varepsilon - \lambda)\kappa = -\mu,$$

where μ is a constant. Another integration yields

$$(16) \quad (\kappa')^2 + \frac{1}{4}\kappa^4 + (\varepsilon - \lambda)\kappa^2 + \mu\kappa = -\nu,$$

where ν is another constant of integration. Thus, the *signature* [5, 22, 25] of a GP-curve is one of the bounded components of an elliptic curve of the following type

$$y^2 + \frac{1}{4}x^4 + (\varepsilon - \lambda)x^2 + \mu x + \nu = 0.$$

We notice that the extremal curves of the the action functional

$$(17) \quad 2\lambda\mathfrak{L}_0 + 2\varepsilon\mu\mathfrak{L}_1 + \mathfrak{L}_2.$$

satisfies (15). In other words, stationary curves of the second order Goldstein–Petrich flow arise as the critical points of linear combinations of the basic distinguished functionals $\mathfrak{L}_0, \mathfrak{L}_1$ and \mathfrak{L}_2 .

REMARK 6. The value $\mu = 0$ yields *elastic curves* in S_ε^2 , i.e. the critical points of the total squared curvature functional with respect to variations with fixed length. These curves have been extensively studied in [2, 9, 17, 18]. If, in addition $\lambda = 0$ the corresponding curves are *free elasticæ*, i.e. the critical points of the total squared curvature functional. Free elasticæ have a special interest in differential geometry because of their interrelations with Willmore surfaces [3, 9, 13, 26].

We note that (15) can be written in terms of a Lax pair. To prove the assertion we set

$$(18) \quad \mathbf{H}_\lambda =: \mathbf{Q} + (\lambda - \varepsilon)\mathbf{K} : \mathbf{J}(\mathbb{R}, \mathbb{R}) \rightarrow \mathfrak{so}_\varepsilon(3),$$

where \mathbf{Q} and \mathbf{K} are defined as in (8) and (9), with $\mathbf{V} = -u_{(1)}$, that is

$$\mathbf{H}_\lambda = \begin{pmatrix} 0 & -\varepsilon(\lambda - \frac{u^2}{2}) & \varepsilon u_{(1)} \\ \lambda - \frac{u^2}{2} & 0 & u_{(2)} + \frac{u^3}{2} - \lambda u \\ -u_{(1)} & -u_{(2)} - \frac{u^3}{2} + \lambda u & 0 \end{pmatrix}.$$

It is then a computational matter to verify that (15) holds if and only if

$$(19) \quad \delta(\mathbf{H}_\lambda|_{j(\kappa)}) = [\mathbf{H}, \mathbf{K}]|_{j(\kappa)}.$$

The main consequence of (19) is the integrability by quadratures of the Golstein-Petrich curves. From the point of view of symplectic geometry, the Lax equation (19) is equivalent to the Noether theorem of the conservation of the momentum map along the extremal curves of the distinguished functionals (17).

3. Numerical solutions and examples

3.1. Numerical solutions

We now show how to implement standard numerical routines in our geometrical setting.

Step 1. Define the curvature ε of S_ε^2 , the coefficients λ and μ of (15), the initial conditions $P_0 = \kappa(0)$, $P_1 = \kappa'(0)$ and the interval $I = (a, b)$:

$$\varepsilon:=1; \quad \lambda:=1-2; \quad \mu:=0.626; \quad P_0:=-0.2; \quad P_1:=2; \quad a:=-8; \quad b:=8;$$

Step 2. Solve (15)

$$\begin{aligned} s[0] &:= \text{NDSolve}[\{k''[t] + \frac{1}{2}k[t]^3 + (\varepsilon - \lambda) * k[t] + \mu == 0, k[0] == P_0, k'[0] == P_1\}, \\ &\{k\}, \{t, a - 0.5, b\}]; \\ K[t_] &:= (\{k[t]\} / s[0])[[1, 1]]; \end{aligned}$$

Step 3. Solve the Frenet–Serret linear system with curvature κ :

$$\begin{aligned} s[1] &:= \text{NDSolve}[\{x'[s] == y[s], x[0] == \varepsilon, y'[s] == K[s] * z[s] - \varepsilon * x[s], \\ &y[0] == 0, z'[s] == -K[s] * y[s], z[0] == 0\}, \{x, y, z\}, \{s, a, b\}]; \end{aligned}$$

```

s[2]:=NDSolve[{x'[s]==y[s],x[0]==0,y'[s]==K[s]*z[s]-ε*x[s],
y[0]==1,z'[s]==-K[s]*y[s],z[0]==0},{x,y,z},{s,a,b}];
s[3]:=NDSolve[{x'[s]==y[s],x[0]==0,y'[s]==K[s]*z[s]-ε*x[s],
y[0]==0,z'[s]==-K[s]*y[s],z[0]==1},{x,y,z},{s,a,b}];
S[1][s_]:=x[s],y[s],z[s]/s[1];
S[2][s_]:=x[s],y[s],z[s]/s[2];
S[3][s_]:=x[s],y[s],z[s]/s[3];

```

Step 4. Define the corresponding GP curve (γ_S =spherical GP curve, γ_E = Euclidean GP curve, γ_H =hyperbolic GP curve)

```

γS[t_]:=S[1][t][[1]][[1]],S[2][t][[1]][[1]],S[3][t][[1]][[1]];
γH[t_]:=S[1][t][[1]][[1]],S[2][t][[1]][[1]],S[3][t][[1]][[1]];
γE[t_]:=S[2][t][[1]][[1]],S[3][t][[1]][[1]];

```

Step 5. Visualize the curvature and the signature

```

SIGNATURE:=ParametricPlot[Evaluate[{K[t],D[K[t],t]},{t,0,b},
PlotPoints→300,AspectRatio→Automatic,
Axes→True,PlotStyle→{Thickness[0.01],Black},ImageSize→{400,400},
Background→GrayLevel[0.8]];
HYPERBOLICCURVE:=Show[Graphics[{GrayLevel[0.6],Disk[{0,0},1]}],
ParametricPlot[Evaluate[γH[s]},{s,a,b},
PlotStyle→{{Thickness[0.01],Black}},Axes→False,
AspectRatio→Automatic,PlotPoints→140,PlotRange→All],
Background→GrayLevel[0.8]];
EUCLIDEANCURVE:=ParametricPlot[Evaluate[γE[s]},{s,a,b},
Background→GrayLevel[0.8],PlotStyle→{{Thickness[0.01],Black}},
Axes→False,AspectRatio→Automatic,PlotPoints→140,
PlotRange→All,ImageSize→{400,400}];
SPHERICALCURVE:=
Show[Graphics3D[{Opacity[0.5],GrayLevel[0.6],Sphere[{0,0,0]}],
Lighting→"Neutral",ParametricPlot3D[Evaluate[γS[s]],
{s,a,b},PlotPoints→300,Boxed→False,AspectRatio→Automatic,
Axes→False,
PlotStyle→{Thickness[0.01],Black}],Boxed→False,
Background→GrayLevel[0.8],
PlotRange→{{-1,1},{-1,1},{-1,1}},ImageSize→{400,400}];

```

3.2. Wave-like Goldstein–Petrich curves

The values

$$\varepsilon = 0, \quad \lambda = 0, \quad \mu \approx 1.103, \quad P_0 = 2, \quad P_1 = 0.2$$

and

$$\varepsilon = 0, \quad \lambda = -1, \quad \mu \approx 1.103, \quad P_0 = 2.1904, \quad P_1 = 0.2$$

give simple wave-like GP curves in \mathbb{R}^2 with symmetry groups \mathbb{Z}_8 and \mathbb{Z}_{11} respectively (see Figure 1). The values

$$\varepsilon = -1, \quad \lambda = 0, \quad \mu \approx -9.987, \quad P_0 = -3, \quad P_1 = 1$$

and

$$\varepsilon = -1, \quad \lambda = 0, \quad \mu \approx -12.05, \quad P_0 = -3, \quad P_1 = 1$$

correspond to simple wave-like GP curves in \mathbb{H}^2 with symmetry groups \mathbb{Z}_6 and \mathbb{Z}_8 respectively (see Figure 2).

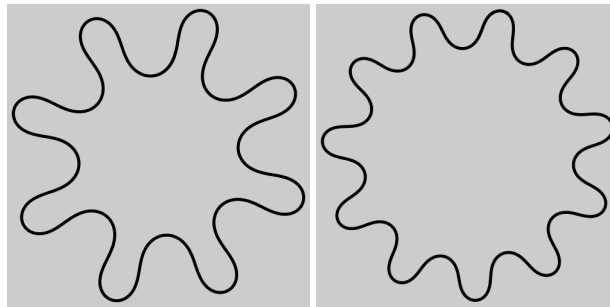


Figure 1: Simple wave-like GP curves in \mathbb{R}^2

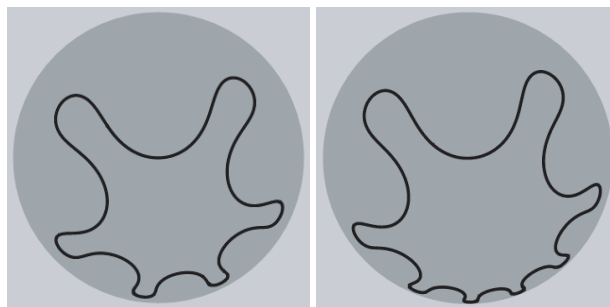


Figure 2: Simple wave-like GP curves in \mathbb{H}^2

3.3. Orbit-like Goldstein–Petrich curves

The values

$$\varepsilon = 0 \quad \lambda = -2 \quad \mu \approx -4.03, \quad P_0 = 2, \quad P_1 = 1,$$

and

$$\varepsilon = 1 \quad \lambda = -1 \quad \mu \approx -4.03, \quad P_0 = 2, \quad P_1 = 1$$

give rise to closed orbit-like GP curves in \mathbb{R}^2 and S^2 with symmetry group \mathbb{Z}_7 (see Figure 3).

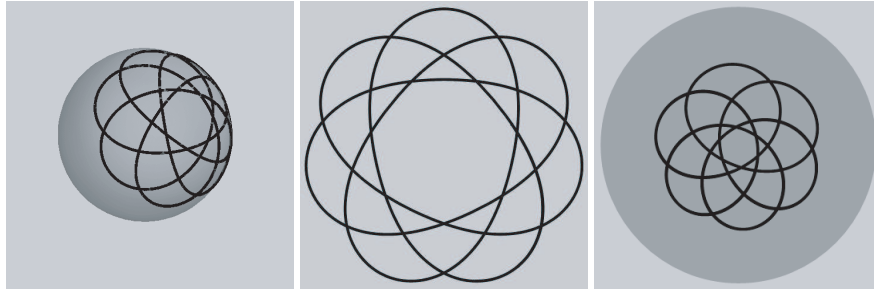


Figure 3: Orbit-like GP curves

Setting

$$\varepsilon = -1 \quad \lambda = 1, \quad \mu \approx -3.8936, \quad P_0 = 2, \quad P_1 = 1$$

we obtain an orbit-like curve in the hyperbolic plane with symmetry group \mathbb{Z}_6 and 24 points of self-intersection (see Figure 3).

4. Spherical free elasticæ

4.1. Spin frames

Consider the special unitary group

$$SU(2) = \{ \mathbf{V} = (V_1, V_2) \in \mathfrak{gl}(2, \mathbb{C}) : \mathbf{V} \cdot \overline{\mathbf{V}}^T = 1, \quad \det(\mathbf{V}) = 1 \}.$$

We take

$$\mathbf{i} = \begin{pmatrix} i & 0 \\ 0 & -i \end{pmatrix}, \quad \mathbf{j} = \begin{pmatrix} 0 & i \\ i & 0 \end{pmatrix}, \quad \mathbf{k} = \begin{pmatrix} 0 & -1 \\ 1 & 0 \end{pmatrix}$$

as standard infinitesimal generators of the Lie algebra $\mathfrak{su}(2)$. We consider the Euclidean inner product

$$\|\mathbf{x}\|^2 = -\frac{1}{2} \text{Tr}(\mathbf{x}^2), \quad \forall \mathbf{x} \in \mathfrak{su}(2).$$

Thus, $(\mathbf{i}, \mathbf{j}, \mathbf{k})$ is a orthogonal basis and

$$(x, y, z) \in \mathbb{R}^3 \rightarrow x\mathbf{i} + y\mathbf{j} + z\mathbf{k} \in \mathfrak{su}(2)$$

gives an explicit identification of $\mathfrak{su}(2)$ with the Euclidean 3-space. Consequently, the 2-dimensional sphere S^2 is identified with $\{ \mathbf{x} \in \mathfrak{su}(2) : \|\mathbf{x}\|^2 = 1 \}$. With these notations at hand, the bundle of spin-frames of S^2 is defined by

$$\pi : \mathbf{V} \in SU(2) \rightarrow \mathbf{V} \cdot \mathbf{i} \cdot \overline{\mathbf{V}}^T \in S^2$$

and, the 2 : 1 spin covering map $SU(2) \rightarrow SO(3)$ is given by

$$\mathbf{V} \in SU(2) \rightarrow (\mathbf{V} \cdot \mathbf{i} \cdot \overline{\mathbf{V}}^T, \mathbf{V} \cdot \mathbf{j} \cdot \overline{\mathbf{V}}^T, \mathbf{V} \cdot \mathbf{k} \cdot \overline{\mathbf{V}}^T) \in SO(3).$$

DEFINITION 1. Let $\gamma: I \rightarrow S^2$ be a smooth curve parameterized by the arc-length and with curvature κ . A spin frame field along γ is a map

$$\mathbf{G} = (\Gamma, \Gamma^*) : I \rightarrow SU(2)$$

such that

$$(20) \quad \gamma = \mathbf{G} \cdot \mathbf{i} \cdot \overline{\mathbf{G}}^T, \quad \Gamma' = \frac{1}{2}(i\kappa\Gamma + \Gamma^*), \quad \Gamma^{*'} = -\frac{1}{2}(\Gamma + i\kappa\Gamma^*).$$

REMARK 7. The spin frame $\mathbf{G} : I \rightarrow SU(2)$ is just a lift to $SU(2)$ of the Frenet frame $\mathbf{F} : I \rightarrow SO(3)$ along γ .

4.2. The monodromy

A spin frame $\mathbf{G} : \mathbb{R} \rightarrow SU(2)$ with non-constant periodic curvature κ and initial condition $\mathbf{G}(0) = \mathbf{1}$ is the solution of linear system with periodic coefficients

$$(21) \quad 2\mathbf{G}' = \mathbf{G} \cdot \begin{pmatrix} i\kappa & -1 \\ 1 & -i\kappa \end{pmatrix}, \quad \mathbf{G}(0) = \mathbf{1}.$$

The *monodromy* of (21) is defined by

$$\mathbf{M} := \mathbf{G}(\omega) \in SU(2),$$

where ω is the minimal period of κ . The two eigenvalues of \mathbf{M} are

$$(22) \quad \mu_{\pm} = \operatorname{Re}(\Gamma_1^1(\omega)) \pm \sqrt{\operatorname{Re}(\Gamma_1^1(\omega))^2 - 1} = e^{\pm 2\pi i \theta} \in S^1,$$

where $\theta \in [0, 1)$. By the Floquet theorem for linear systems of o.d.e with periodic coefficients (cfr. [1]) it follows that \mathbf{G} is a periodic solution of (21) if and only if

$$\theta = p/q \in [0, 1), \quad p, q \in \mathbb{N}, \quad \gcd(p, q) = 1.$$

DEFINITION 2. The minimal period of the spin frame \mathbf{G} is $\ell_s = q\omega$ and the minimal period ℓ of the corresponding spherical curve $\gamma = \pi \circ \mathbf{G}$ can be either ℓ_s or else $\ell_s/2$. In the first case we say that γ is a spherical curve with spin 1 while in the second case we say that γ is a spherical curve with spin $1/2$.

REMARK 8. For a spherical curve of spin 1 the integer q is odd and gives the order of its symmetry group. For a curve of spin $1/2$ the integer q is even and the order of the symmetry group is $q/2$.

4.3. The monodromy of free elasticae in S^2

The curvature of a spherical free elastica satisfies

$$(23) \quad \kappa'' + \frac{1}{2}(\kappa^2 + 2)\kappa = 0.$$

The general periodic solution of (23) is

$$(24) \quad \kappa(s, \lambda) = 2\sqrt{\frac{\lambda}{1-2\lambda}} \text{JacobiCN}\left(\frac{s}{\sqrt{1-2\lambda}}, \lambda\right)$$

where $\lambda \in (0, 1/2)$ and $\text{JacobiCN}(z, \lambda)$ denotes the Jacobi cn-function with modulus $\sqrt{\lambda}$. The minimal period of $k(s, \lambda)$ is given by

$$(25) \quad \omega_\lambda = 4\sqrt{1-2\lambda} \text{EllipticK}(\lambda),$$

where

$$\text{EllipticK}(\lambda) = \int_0^{\pi/2} \frac{d\theta}{\sqrt{1-\lambda \sin^2(\theta)}}.$$

For each $\lambda \in (0, 1/2)$ we denote by

$$\mathbf{G} : \mathbb{R} \times (0, 1/2) \rightarrow \mathbf{G}(s, \lambda) \in \text{SU}(2)$$

the spin frame field with curvature $\kappa(-, \lambda)$ and initial condition $\mathbf{G}_\lambda(0) = \mathbf{1}$. We then define the *Floquet map*

$$(26) \quad m : \lambda \in (0, 1/2) \rightarrow m(\lambda) \in S^1$$

by

$$m(\lambda) = \text{Re}(\Gamma_1^1(\omega_\lambda, \lambda)) + \sqrt{\text{Re}(\Gamma_1^1(\omega_\lambda, \lambda))^2 - 1} = e^{2\pi i \theta(\lambda)},$$

where $\theta(\lambda) \in (0, 1)$. The Floquet map can be computed in closed form by means of the Heuman’s Lambda function [19] or with numerical methods. We now exhibit the code of the numerical evaluation of the Floquet map:

Step 1. Define $\kappa(s, \lambda)$, the period ω_λ :

$$\begin{aligned} \text{K}[t_ , \lambda_] &:= \sqrt{\frac{4*\lambda}{1-2*\lambda}} \text{JacobiCN}\left[\frac{t}{\sqrt{(1-2*\lambda)}}, \lambda\right]; \\ \omega[\lambda_] &:= \left(4 * \sqrt{(1-2*\lambda)}\right) * \text{EllipticK}[\lambda]; \end{aligned}$$

Step 2. Solve numerically the linear system (20) :

$$\begin{aligned} \text{A}[1] &:= \{1, 0\}; \\ \text{A}[2] &:= \{0, 1\}; \\ \text{sol}[1][\lambda_] &:= \end{aligned}$$

```

NDSolve[{x'[t] == (1/2)(i * K[t, λ] * x[t] + y[t]), x[0] == A[1][[1]],
y'[t] == (1/2)(-i * K[t, λ] * y[t] - x[t]), y[0] == A[2][[1]]}, {x, y},
{t, -0.5, ω[λ]}];
sol[2][λ_]:=
NDSolve[{x'[t] == (1/2)(i * K[t, λ] * x[t] + y[t]), x[0] == A[1][[2]],
y'[t] == (1/2)(-i * K[t, λ] * y[t] - x[t]), y[0] == A[2][[2]]}, {x, y},
{t, -0.5, ω[λ]}];
S[1][t_, λ_]:= {x[t], y[t]}/.sol[1][λ];
S[2][t_, λ_]:= {x[t], y[t]}/.sol[2][λ];
M[t_, λ_]:= Transpose[{S[1][t, λ][[1]][[1]], S[2][t, λ][[1]][[1]]},
{-Conjugate[S[2][t, λ][[1]][[1]]], Conjugate[S[1][t, λ][[1]][[1]]]}];
Monodromy[λ_]:= M[ω[λ], λ];
μ[λ_]:= Re[S[1][ω[λ], λ][[1]][[1]]] + √Re[S[1][ω[λ], λ][[1]][[1]]]^2 - 1;

```

Step 3. Compute the monodromy and the Floquet map

```

M[t_, λ_]:= Transpose[{S[1][t, λ][[1]][[1]], S[2][t, λ][[1]][[1]]},
{-Conjugate[S[2][t, λ][[1]][[1]]], Conjugate[S[1][t, λ][[1]][[1]]]}];
Monodromy[λ_]:= M[ω[λ], λ];
μ[λ_]:= Re[S[1][ω[λ], λ][[1]][[1]]] + √Re[S[1][ω[λ], λ][[1]][[1]]]^2 - 1;

```

Step 4. Plot and visualize the image of the Floquet map and the graph of its real part

```

α[λ_]:= {Re[μ[λ]], Im[μ[λ]]};
FLOQUET:= Show[Graphics[{GrayLevel[0.8], Disk[{0, 0}]}],
ParametricPlot[α[λ], {λ, 0, 0.499}, Background → GrayLevel[0.8],
PlotStyle → {{Thickness[0.02], Black}},
PlotRange → {{-1.2, 1.2}, {-1.2, 1.2}}, PlotPoints → 200,
AspectRatio → Automatic, Axes → False]];

```

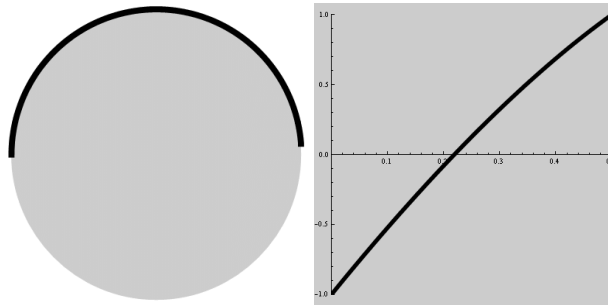


Figure 4: The Floquet map and its real part

Plotting the image of the Floquet map and the graph of its real part (Figure 4) we infer that m is a bijection of $(0, 1/2)$ onto $S_+^1 = \{e^{it} : t \in (0, \pi)\}$. We set

$$(27) \quad \phi : \tau \in (0, 1/2) \rightarrow m^{-1}(e^{2\pi i \tau}) \in (0, 1/2)$$

and, for every $\tau \in (0, 1/2)$ we let γ_τ be the free elastica with parameter $\lambda = \phi(\tau)$. Summarizing the discussion, we have

PROPOSITION 1. *The curve γ_τ is a closed free elastica if and only if $\tau = p/q$, where $p, q \in \mathbb{N}$, $\gcd(p, q) = 1$ and $0 < p/q < 1/2$.*

To evaluate $\phi(p/q)$ we proceed as follows : first we note that $\phi(p/q)$ is the unique zero of the function

$$\Phi_{p/q} : \lambda \in (0, 1/2) \rightarrow \|m(\lambda) - e^{2\pi i \frac{p}{q}}\|^2 \in \mathbb{R}^+.$$

Plotting the graph of $\Phi_{p/q}$ we have a first rough estimate of the location of $\phi(p/q)$ (Figure 5).

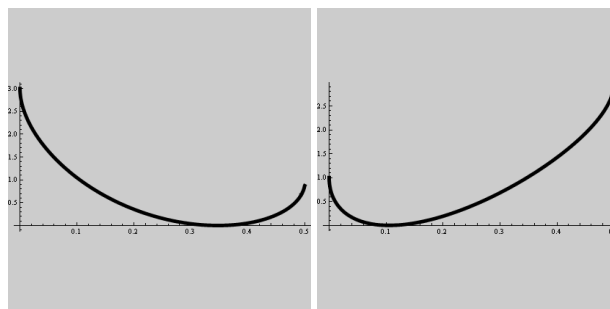


Figure 5: The graphs of $\Phi_{1/6}$ and $\Phi_{1/3}$

We then choose an initial value $\lambda_1 \in (0, 1/2)$ sufficiently near to $\phi(p/q)$ and we start to search the minimum λ_2 of $\Phi_{p/q}$ inside the interval $[\lambda_1 - \delta, \lambda_1 + \delta]$, among a finite set D_1 of k elements. We repeat the procedure by taking λ_2 as a new initial value and searching for the minimum of $\Phi_{p/q}$ in the interval $[\lambda_2 - \delta/2, \lambda_2 + \delta/2]$ among a finite set D_2 of $2k$ elements. Proceeding recursively we find, after n steps, a value λ_n which approximates $\phi(p/q)$ with the desired precision. In practice, a good approximation of $\phi(p/q)$ is given by any λ_n such that $\Phi_{p/q}(\lambda_n) < 10^{-h}$, with $h \geq 8$.

Step 1. Compute $\Phi_{p/q}$

$$\Psi[\lambda_-, p_-, q_-] := \text{Abs} \left[\mu[\lambda] - \text{Exp} \left[2 * \text{Pi} * i * \frac{p}{q} \right] \right]^2;$$

and visualize its graph

```
DISTRIBUTION:=Plot[Ψ[λ, p, q], {λ, -3, 3},
PlotStyle → {{Thickness[0.01], Black}}, PlotRange → All,
PlotPoints → 200, AspectRatio → 1/2, Axes → True, ImageSize → {400, 250},
Background → GrayLevel[0.8], PlotRange → {{-3, 3}, {0, 4}}]
```

Step 2. Search of the approximated values of $\min(\Phi_{p/q})$:

```

p:=1;q:=4;τ1:=0.4;
internalparameter[1]:=1/12;
internalparameter[2]:=20;
steps:=8;
Q[y_,δ_,k_]:=First[Sort[Table[{Ψ[λ,p,q],λ},{λ,y-δ,y+δ,1/k}]]];
S[1,y_,δ_,k_]:=Q[y,δ,k];
S[m_,y_,δ_,k_]:=S[m-1,S[m-1,y,δ,k][[2]],δ/(2m-1),k*(2m-1)];
S[steps,τ1,internalparameter[1],internalparameter[2]];

```

4.4. Examples

The approximated values of $\phi(1/2h)$, for $h = 2, \dots, 7$ are given by

$$\phi(1/4) \approx 0.219105, \quad \phi(1/6) \approx 0.347017, \quad \phi(1/8) \approx 0.406183,$$

and by

$$\phi(1/10) \approx 0.437212, \quad \phi(1/12) \approx 0.455251, \quad \phi(1/14) \approx 0.466582.$$

The corresponding free elasticæ are reproduced in Figures 6 and 7. All these curves are simple, with symmetry groups \mathbb{Z}_h and subdivide S^2 into two congruent pieces.

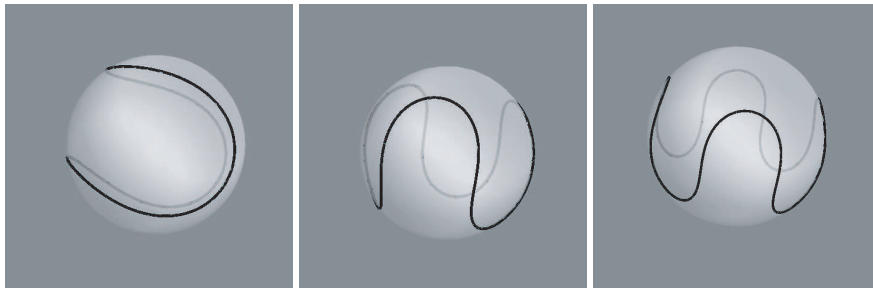


Figure 6: The free elasticæ $\gamma_{1/2h}$, $h = 2, 3, 4$

The first approximated values of $\phi(p/7)$ are

$$\phi(1/7) \approx 0.381729, \quad \phi(2/7) \approx 0.166961, \quad \phi(3/7) \approx 0.0201934.$$

The associated free elasticæ are closed, with symmetry group \mathbb{Z}_7 and with 7, 21 and 35 points of self-intersection, respectively. The curves are reproduced in Figure 8.

The first three approximated values of $\phi(p/16)$ are

$$\phi(3/16) \approx 0.315366, \quad \phi(5/16) \approx 0.130811, \quad \phi(7/16) \approx 0.0015496.$$

The associated free elasticæ are closed, with symmetry group \mathbb{Z}_8 and with 8, 32 and 58 points of self-intersection, respectively. The curves are reproduced in Figure 9.

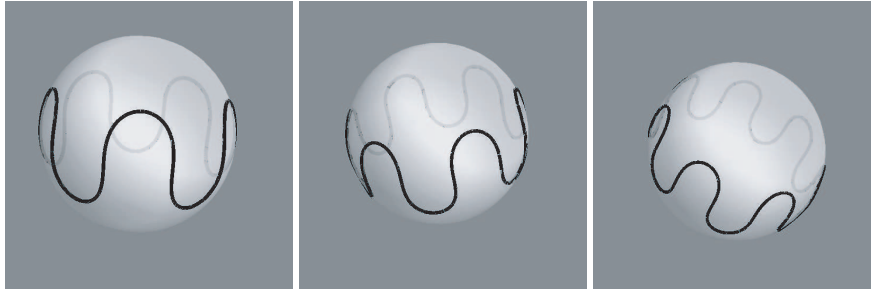


Figure 7: The free elastica $\gamma_{1/2h}$, $h = 5, 6, 7$

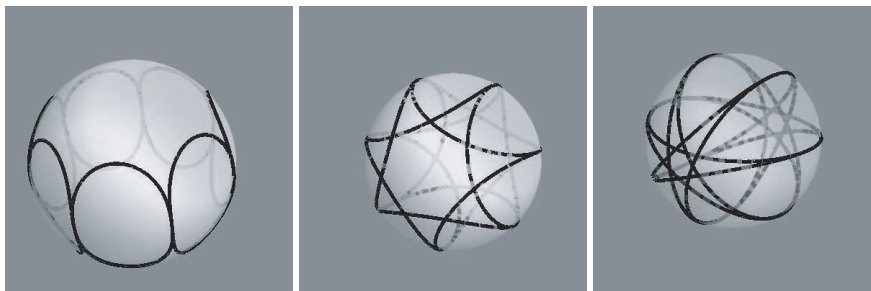


Figure 8: The free elastica $\gamma_{p/7}$, $p = 1, 2, 3$

4.5. Conclusions

The examples above and the evidence of other numerical experiments suggest the following geometrical facts*.

PROPOSITION 2. *Let $\gamma_{p/q}$ be a closed free elastica in S^2 with $p, q \in \mathbb{N}$, $p/q \in (0, 1/2)$ and $\gcd(p, q) = 1$, then*

- *if q is even ($q = 2q'$) the elastica $\gamma_{p/2q'}$ has spin $1/2$, symmetry group $\mathbb{Z}_{q'}$ and possesses $(p - 1)q'$ points of self-intersection;*
- *if q is odd ($q = 2q' + 1$), the elastica $\gamma_{p/(2q'+1)}$ has spin 1 , symmetry group $\mathbb{Z}_{2q'+1}$ and possesses $(2p - 1)q$ points of self-intersection;*
- *$\gamma_{p/q}$ is a simple curve if and only if $p = 1$ and $q \in 2\mathbb{N}$.*

*See ref. [18] for similar results in the case of free elasticae in the Poincaré disk.



Figure 9: The free elastica $\gamma_{p/16}$, $p = 3, 5, 7$

4.6. Embedded Pinkall's tori

If $\mathbf{G} : I \rightarrow \mathrm{SU}(2)$ is a spin frame field of a unit-speed spherical curve $\gamma : I \rightarrow S^2$ with curvature κ then the map

$$f : (s, \vartheta) \in I \times \mathbb{R} \rightarrow e^{\frac{i}{2}(\vartheta - \int \kappa(u) du)} \mathbf{G}(s) \in S^3 \subset \mathbb{C}^2$$

is a flat immersion into the unit 3-sphere which is called the *Hopf immersion* associated to γ . The first and second fundamental forms of f are

$$I = \frac{1}{4}(ds^2 + d\vartheta^2), \quad II = \frac{1}{2}(\kappa ds^2 - dsd\vartheta).$$

Thus, κ gives the mean curvature H of the corresponding Hopf immersion. Therefore, if γ is a Goldstein–Petrich curve the mean curvature of the Hopf immersion satisfies

$$(28) \quad \Delta(H) + 2\left(H^2 + \frac{a}{b} - K\right)H = p,$$

where Δ is the Laplace–Beltrami operator of the induced Riemannian metric and a, b, p are constants. Immersions satisfying (28) are the critical points of the Hooke's energy

$$E(f) = \int (bH^2 + a)dA.$$

They are known as *elastic surfaces* [13]. Physically, a is the surface tension, b the bending energy and p is the pressure. The case $a = b = 1$ and $p = 0$ has a particular geometrical interest; the curve γ is a free elastica and f parameterizes a *Willmore surface*. One of the key features of Willmore immersions is their invariance with respect to the group of Möbius (conformal) transformations of S^3 . Using this construction and the results of Langer–Singer [17], U. Pinkall [26] discovered the first examples of embedded Willmore tori which are not Möbius equivalent to any minimal surface in S^3 . The stereographic projections of these surfaces are called *Pinkall's tori* of \mathbb{R}^3 . Our experiments show that Pinkall tori are associated to the free elastic curves $\gamma_{1/2n}$, $n \in \mathbb{N}$ and $n > 2$. If we choose appropriately the pole of the stereographic projection, the Pinkall surface defined by $\gamma_{1/2n}$ has a symmetry group isomorphic to \mathbb{Z}_n (see Figure 10).

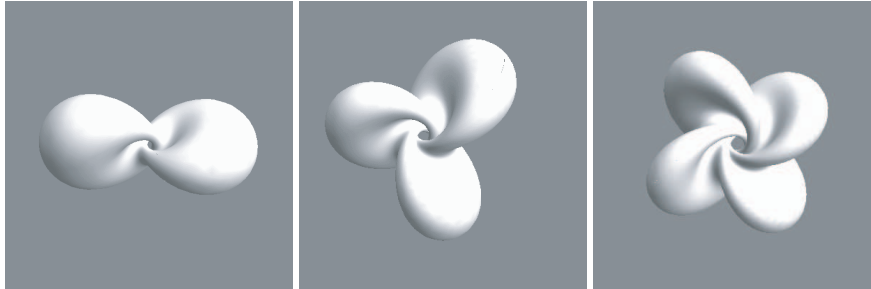


Figure 10: Pinkall's tori with symmetry groups \mathbb{Z}_2 , \mathbb{Z}_3 and \mathbb{Z}_4

References

- [1] ARNOLD V.I., *Geometrical Methods in the Theory of Ordinary Differential Equations*, Grundlehren der Mathematischen Wissenschaften 250, Springer Verlag, New York (1988).
- [2] BRYANT R. AND GRIFFITHS P., *Reduction for constrained variational problems and $\int \kappa^2 ds$* , Amer. J. Math. **108** (1986), 525–570.
- [3] BHOLE C. AND PETERS G. P., *Bryant surfaces with smooth ends*, arXiv:math/0411480v3.
- [4] BROWER R. C., KESSLER D. A., KOPLIK J. AND LEVINE H., *Geometrical models of interface evolution*, Phys. Rev. A **29** (1984), 1335–1342.
- [5] CALABI E., OLVER P. J., SHAKIBAN C., TANNENBAUM A. AND HAKER S., *Differential and numerically invariant signature curves applied to object recognition*, Int. J. Comput. Vis. **26** (1998), 107–135.
- [6] K.-S. CHOU AND C. QU, *Integrable equations arising from motions of plane curves*, Phys. D **163** (2002), 9–33.
- [7] K.-S. CHOU AND C. QU, *Integrable equations arising from motions of plane curves. II*, J. Nonlinear Sci. **13** (2003), 487–517.
- [8] DOLIWA A. AND SANTINI P.M., *An elementary geometric characterization of the integrable motions of a curve*, Phys. Lett. A **85** (1992), 339–384.
- [9] GRIFFITHS P., *Exterior differential systems and the calculus of variations*, Birkhäuser, Boston 1982.
- [10] GRANT J. AND MUSSO E., *Coisotropic variational problems*, J. Geom. Phys. **50** (2004), 303–338.
- [11] GOLDSTEIN R. E. AND PERTICH D. M., *The Korteweg-de Vries hierarchy as dynamics of closed curves in the plane*, Phys. Rev. Lett. **67** 23 (1991), 3203–3206.
- [12] HASHIMOTO H., *A soliton on a vortex filament*, J. Fluid Mech. **51** (1972), 477–485.
- [13] HSU L., KUSNER R. AND SULLIVAN J., *Minimizing the squared mean curvature integral for surfaces in space forms*, Experiment. Math. **1** (1992), 191–207.
- [14] LAMB G. L., *Solitons and motion of helical curves*, Phys. Rev. Lett. **37** 5 (1976), 235–237.
- [15] LAMB G. L., *Solitons on moving space curves*, J. Math. Phys. **18** 8 (1977), 1654–1661.
- [16] LANGER J. L. AND PERLINE R., *Curve motion inducing modified Korteweg-de Vries systems*, Phys. Lett. A **239** (1998), 36–40.
- [17] LANGER J. L. AND SINGER D. A., *The total squared curvature of closed curves*, J. Differential Geom. **20** (1984), 1–22.

- [18] LANGER J. L. AND SINGER D. A., *Curves in the hyperbolic plane and mean curvature of tori in 3-space*, Bull. Lond. Math. Soc. **16** (1984), 531–534.
- [19] LAWDEN D.F., *Elliptic Functions and Applications*, Series Applied Mathematical Science **80** Springer, New York 1989.
- [20] MARÍ BEFFA G., *Poisson Brackets associated to the conformal geometry of curves*, Trans. Amer. Math. Soc. **357** 7 (2004), 2799–2872.
- [21] MARÍ BEFFA G., *Projective-type differential invariants and geometric curve evolutions of KdV-type in flat homogenous spaces*, Ann. Inst. Fourier (Grenoble) **58** (2008), 1295–1335.
- [22] MUSSO E. AND NICOLODI L., *Invariant signatures of closed planar curves*, J. Math. Imaging Vision **43** 1 (2009).
- [23] NAKAYAMA K., SEGUR H. AND WADATI M., *Integrability and the motion of curves*, Phys. Rev. Lett. **69** 18 (1992), 2603–3606.
- [24] OLVER P. J., *Equivalence, Invariants and Symmetry*, Cambridge University Press 1995.
- [25] OLVER P. J., *Invariant signatures*, Breckenridge, March 2007; Seminars and Conference Talks at <http://www.math.umn.edu/~olver>.
- [26] PINKALL U., *Hopf tori in S^3* , Invent. Math. **81** (1985), 376–386.

AMS Subject Classification: 53A40, 58A15 (53D10, 58A17)

Emilio MUSSO,
Dipartimento di Matematica, Politecnico di Torino,
Corso Duca degli Abruzzi 24, 10129, Torino, ITALIA
e-mail: emilio.musso@polito.it

Lavoro pervenuto in redazione il 30.11.2009